BMB
Reports

BMB Rep. 2019; 52(8): 526-531
www.bmbreports.org

Akap12beta supports asymmetric heart development via modulating the Kupffer's vesicle formation in zebrafish

Jeong-gyun Kim[1], *Hyun-Ho Kim*[1,2] *& Sung-Jin Bae*[1,3,*]

[1]College of Pharmacy and Research Institute of Pharmaceutical Sciences, Seoul National University, Seoul 08826, [2]Biological and Medical Device Evaluation Team, Korea Testing & Research Institute, Gwacheon 13810, [3]Korean Medicine Research Center for Healthy Aging, Pusan National Univerity, Yangsan 50612, Korea

The vertebrate body plan is accomplished by left-right asymmetric organ development and the heart is a representative asymmetric internal organ which jogs to the left-side. Kupffer's vesicle (KV) is a spherical left-right organizer during zebrafish embryogenesis and is derived from a cluster of dorsal forerunner cells (DFCs). Cadherin1 is required for collective migration of a DFC cluster and failure of DFC collective migration by Cadherin1 decrement causes KV malformation which results in defective heart laterality. Recently, loss of function mutation of A-kinase anchoring protein 12 (*AKAP12*) is reported as a high-risk gene in congenital heart disease patients. In this study, we demonstrated the role of *akap12β* in asymmetric heart development. The *akap12β*, one of the *akap12* isoforms, was expressed in DFCs which give rise to KV and *akap12β*-deficient zebrafish embryos showed defective heart laterality due to the fragmentation of DFC clusters which resulted in KV malformation. DFC-specific loss of *akap12β* also led to defective heart laterality as a consequence of the failure of collective migration by *cadherin1* reduction. Exogenous *akap12β* mRNA not only restored the defective heart laterality but also increased *cadherin1* expression in *akap12β* morphant zebrafish embryos. Taken together, these findings provide the first experimental evidence that *akap12β* regulates heart laterality via *cadherin1*. [BMB Reports 2019; 52(8): 526-531]

INTRODUCTION

Kupffer's vesicle (KV) is a spherical left-right organizer which appears transiently during an embryonic stage in zebrafish (1). KV originates from a cluster of dorsal forerunner cells (DFCs). Cadherin1 (Cdh1)-mediated adherens junctions sustain cell cluster formation between the adjacent DFCs and a cluster of DFCs actively migrates towards the vegetal pole to form KV (2). Then, migrated DFCs attach to the overlying surface epithelium and become polarized to construct a rosette-like structure which contains the lumen at the apical point (3). Finally, cilia-formed and fluid-filled KV expands the internal lumen and motile cilia generate fluid flow in a counterclockwise direction to evoke asymmetric signal(s) such as Nodal, Lefty, and Pitx2 (1).

The vertebrate body plan is accomplished by left-right asymmetric organ development. The heart is a representative asymmetric internal organ which jogs to the left-side and proper positioning during embryonic development is crucial for its function (4). Accordingly, about ~1% of newborn babies suffer from congenital heart disease (CHD), which has high mortality (5). Dextrocardia, a rare condition in which the apex of the heart is located on the right side of the body, comprises a CHD case with heterotaxy which is often accompanied by asymmetric defects such as a left-sided liver and a right-sided stomach (6).

A-kinase anchoring protein 12 (AKAP12) is a member of the AKAP family proteins, which bind to the regulatory subunit of protein kinase A (PKA) and holoenzyme localizes to specific locations within the cell. Besides PKA, AKAP12 displays diverse docking sites for protein kinase C, calmodulin, cyclins, β-1,4-galactosyltransferase, protein phosphatases, the non-receptor tyrosine kinase Src, and β2-adrenergic receptor. In addition, AKAP12 consists of three polybasic domains, four nuclear localization signals, and a nuclear exclusion domain. Therefore, AKAP12 plays various roles in many biological processes including cell migration, cell cycle regulation, barriergenesis, tumor progression, and wound healing (7). Our group previously reported that AKAP12 regulates the blood-brain and blood-retinal barrier (8, 9). This barriergenic property of AKAP12 is also applied to the repair of the central nervous system (CNS) after injury. AKAP12 is strongly expressed in the fibrotic scar during the CNS repair process where it mediates barrier functions (10). Moreover, we and other group reported that *akap12* is involved in mesodermal cell shape change, muscle progenitor cell migration and regulation of vascular integrity in zebrafish (11-13).

*Corresponding author. Tel: +82-51-510-8434; Fax: +82-51-510-8437; E-mail: Dr.NowOrNever@pusan.ac.kr

https://doi.org/10.5483/BMBRep.2019.52.8.111

Received 15 April 2019, Revised 10 May 2019, Accepted 3 June 2019

Keywords: AKAP12, Asymmetric development, Heart laterality, Kupffer's vesicle (KV), Zebrafish

ISSN: 1976-670X (electronic edition)

Previous *AKAP12* studies did not focus on the differential role of the two *AKAP12* isoforms, *AKAP12α* and *AKAP12β*. Although they only have a small difference in the N-terminal region (less than 5%), each *AKAP12* isoform has an independent promoter (14) and shows distinct spatiotemporal mRNA expression during embryogenesis (12, 13). Interestingly, a recent study identified *AKAP12* as a loss-of-function mutated gene in CHD patients, which has not been reported in previous reports (15). Here, we demonstrate that *akap12β*, not *akap12α*, is expressed in DFCs and that loss of *akap12β* leads to defective heart laterality due to decreased *cdh1* expression. This report provides the first experimental evidence of a heart laterality regulatory mechanism by *akap12β*, which might also play a role in human heart heterotaxy.

RESULTS

Akap12β is the major isoform of *akap12* during KV development in zebrafish

Akap12α and *akap12β* are two known isoforms of *akap12* in zebrafish (Fig. 1A). During embryonic development, each isoform is differentially regulated due to a distinct promoter region (Fig. 1A, B). The expression of *akap12β* was first observed in the sphere stage, and that of *akap12α* was initiated in the bud stage, later than *akap12β*. Interestingly, *akap12β* morpholino (MO) injection significantly reduced the expression of *pan-akap12* at 75% epiboly stage, while *akap12α* MO injection did not affect the *pan-akap12* expression (Fig. 1C, D).

Next, we investigated the spatiotemporal expression of *akap12* by *in situ* hybridization (ISH) (Fig. 1E-G). Mesodermal cells highly expressed *akap12* mRNA as previously reported (11). Interestingly, *akap12* was expressed in *sox17*-positive DFCs, known as the progenitor cells of KV. The observed *akap12* was suggested to be *akap12β*, as *sox17*-positive DFCs, which originate from non-involuting endocytic marginal cells, are present at the 75% epiboly stage (Fig. 1E, F). Moreover, two color ISH for *akap12* and *dand5*, the marker of KV, revealed that *akap12* expression in KV was not detected at the 6 somite stage (ss) when KV formation by DFC collective migration is completed (Fig. 1G). Taken together, *akap12β*, but not *akap12α*, was transiently expressed in KV ascendant cells when the cluster of DFCs underwent collective migration.

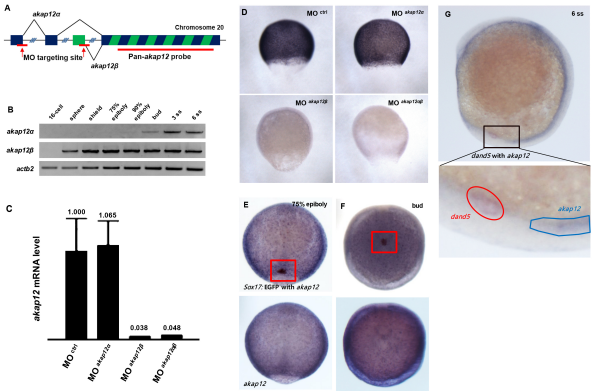

Fig. 1. KV lineage cells express *akap12β* in zebrafish. (A) The genomic locus of *akap12* in zebrafish. (B) RT-PCR analysis of two *akap12* isoforms. (C) qRT-PCR analysis of *pan-akap12* mRNA at 75% epiboly stage in control, *akap12α*, *akap12β*, and *akap12αβ*-double morphants. (D) ISH images of *pan-akap12* at 75% epiboly stage in control, *akap12α*, *akap12β*, and *akap12α* and *β*-double morphants. (E, F) ISH for *pan-akap12* (blue) within immunostained *sox17*:EGFP-positive DFCs (brown) at 75% epiboly (E) or bud stage (F) was marked by a red rectangle. (G) Two color ISH for *pan-akap12* and *dand5* at 6 ss.

Heart laterality is disrupted in *akap12β* morphants

Specific expression of *akap12β* in KV lineage cells motivated us to investigate whether *akap12β* regulates the left-sided heart orientation via fine-tuning the KV formation in zebrafish. First, the positioning of the heart was investigated by ISH for *cmlc1* in *akap12β* morphants. *Akap12β* morphants exhibited mesocardia (~20%) and dextrocardia (~12%), while control morphants showed normal heart laterality (Fig. 2A, B). Then, we evaluated KV formation in *akap12β* morphants by ISH for

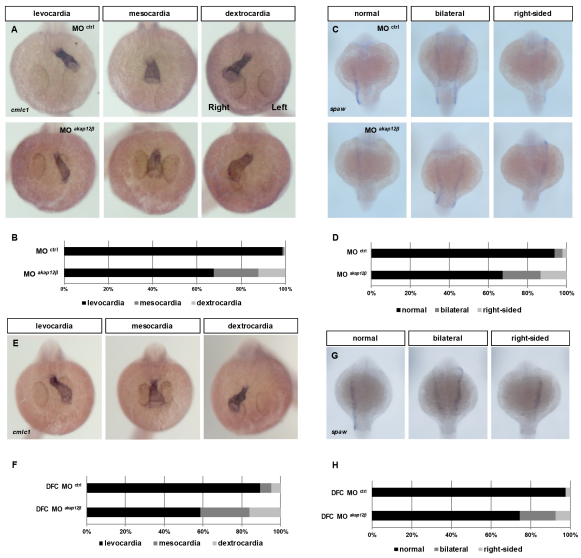

Fig. 2. Knockdown of *akap12β* disrupts organ laterality. (A) Visualization of the heart by ISH for *cmlc1* in 30 hpf embryos of control and *akap12β* morphants. (B) Stacked bar graph (control morphants; n = 154, *akap12β* morphants; n = 143). (C) Representative images of *spaw* by ISH in 18 ss embryos of control and *akap12β* morphants. (D) Stacked bar graph (control morphants; n = 174, *akap12β* morphants; n = 195). (E) Visualization of the heart by ISH for *cmlc1* in 30 hpf embryos of DFC-specific morphants. (F) Stacked bar graph (DFC control morphants; n = 85, DFC *akap12β* morphants; n = 94). (G) Representative images of *spaw* by ISH for *cmlc1* in 30 hpf embryos of DFC-specific morphants. (H) Stacked bar graph (DFC control morphants; n = 45, DFC *akap12β* morphants; n = 67).

spaw, the nodal-related gene and a novel marker for KV, as the abnormal KV development is a frequent cause of disorienting heart laterality. Bilateral (19%) and right-sided (13%) *spaw* expression were observed in *akap12β* morphants while aberrant *spaw* expression was observed in only 6% of the control morphants (Fig. 2C, D).

To investigate whether the specific downregulation of *akap12β* in the KV lineage cells such as DFCs also disrupts heart laterality, the *akap12β* MO was injected into the yolk at the 128 to 512-cell stage (DFC MO) for exclusive reduction of *akap12β* in the KV lineage cells including DFCs (16). DFC-specific injected MO is restricted in the boundary between the blastomeres and yolk where the KV lineage cells exist since the marginal blastomeres are connected to the yolk cell by a cytoplasmic bridge (Supplementary Fig. S1). Disrupted heart laterality (~41%) and aberrant *spaw* expression (~25%) were also observed in DFC-specific *akap12β* morphants, whereas low rate defects were identified in DFC control morphants (Fig. 2E-H).

Akap12β regulates collective migration of DFCs

Next, we validated the notochordal expression of *lefty1*, which functions as the midline molecular barrier to restrict nodal activity to the left lateral plate mesoderm (17). However, normal expression of *lefty1* was observed in the notochord of both control and *akap12β* morphants, regardless of dorsal curvature (Fig. 3A, B). Then, we examined *dand5* expression, which is a molecular barrier of *spaw* by surrounding KV. The control morphants showed mostly normal *dand5* expression with a horseshoe shape, however, discontinuous *dand5* expression was observed in ~58% of *akap12β* morphants (Fig. 3C, D). Moreover, a *sox17*:EGFP-positive DFC cluster, which gives rise to the KV, was identified as fragmentation of DFC clusters in 30% of DFC *akap12β* morphants, while minimal DFC fragmentation was observed in only ~1% of DFC control morphants (Fig. 3E, F). Then, we confirmed the DFC fragmentation in DFC *akap12β* morphants by ISH for *foxj1a* at 75% epiboly stage. Fragmentation of *foxj1a*-positive DFC clusters was observed in ~39% of DFC *akap12β* morphants, while a single non-fragmented DFC cluster was identified in DFC control morphants (Fig. 3G, H).

Taken together, these data suggest that reduced *akap12β* expression in DFCs results in the disruption of asymmetric signals and heart laterality due to failure of DFC collective

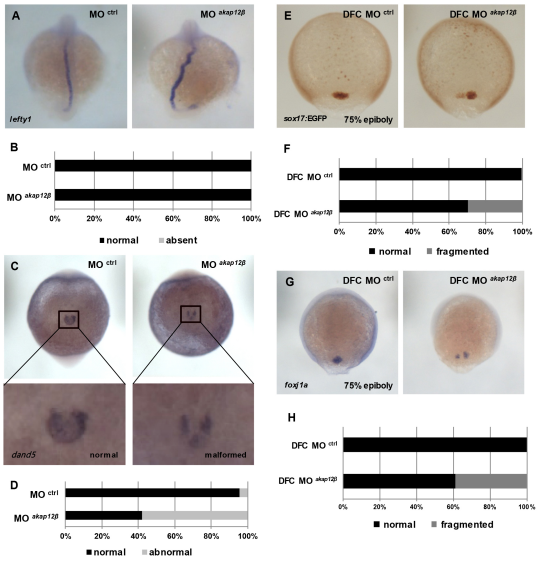

Fig. 3. Failure of collective migration of DFCs in *akap12β* morphants. (A) Visualization of *lefty1* by ISH in 18 ss embryos of control and *akap12β* morphants. (B) Stacked bar graph (control morphants; n = 74, *akap12β* morphants; n = 92). (C) Representative images of *dand5* by ISH in 6 ss embryos of control and *akap12β* morphants. (D) Stacked bar graph (control morphants; n = 86, *akap12β* morphants; n = 110). (E) Visualization of DFC clusters by immunostaining of *sox17*:EGFP in 75% epiboly embryos of DFC-specific morphants. (F) Stacked bar graph (DFC control morphants; n = 82, DFC *akap12β* morphants; n = 77). (G) Representative images of DFC clusters by ISH for *foxj1a* in 75% epiboly embryos of DFC-specific morphants. (H) Stacked bar graph (DFC control morphants; n = 22, DFC *akap12β* morphants; n = 36).

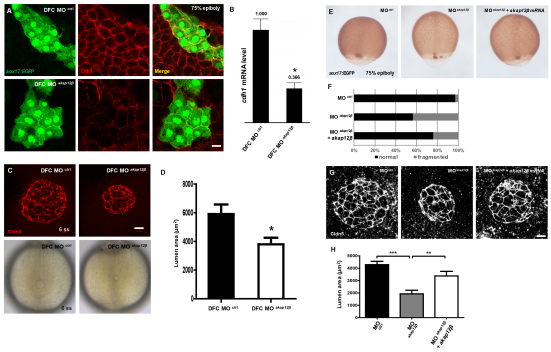

Fig. 4. Malformation of KV integrity in *akap12β* morphants and restoration of defective phenotypes in *akap12β* morphants by exogenous *akap12β* mRNA. (A) Immunostaining of Cdh1 and *sox17*:EGFP in 75% epiboly embryos of DFC control and *akap12β* morphants. Scale bar, 10 μm. (B) qRT-PCR analysis of *cdh1* mRNA in 75% epiboly embryos of DFC control and *akap12β* morphants. (C) Representative images of Cldn5α-immunostained KV lumen (upper) and whole embryo (lower) in 6 ss embryos of DFC control and *akap12β* morphants. Scale bar, 20 μm. (D) The lumen area surrounded by Cldn5α is shown as the means ± SD; *P < 0.05, (DFC control morphants; n = 10, DFC *akap12β* morphants; n = 13). (E) Visualization of DFC clusters by immunostaining of *sox17*:EGFP in 75% epiboly embryos of control, *akap12β*, and *akap12β* mRNA-injected *akap12β* morphants. (F) Stacked bar graph (control morphants; n = 32, *akap12β* morphants; n = 30, *akap12β* mRNA-injected *akap12β* morphants; n = 35). (G) Visualization of KV lumen by immunostaining for Cldn5α in 6 ss embryos of control, *akap12β*, and *akap12β* mRNA-injected *akap12β* morphants. Scale bar, 20 μm. (H) The lumen area surrounded by Cldn5α is shown as the means ± SD; ***P < 0.001, **P < 0.01, (control morphants; n = 10, *akap12β* morphants; n = 10, *akap12β* mRNA-injected *akap12β* morphants; n = 11).

migration.

Reduction of cdh1 by akap12b knockdown disrupts DFC cluster integrity

Fragmented DFC clusters are the symbolic phenotype of disrupted cell collectivity between DFCs which is maintained by Cdh1-based adherence junction (18). Thus, we evaluated Cdh1 expression in *akap12β* morphants by immunostaining at 75% epiboly stage. DFC control morphants showed high Cdh1 expression at intercellular surfaces between the DFCs. However, DFC *akap12β* morphants displayed significantly reduced Cdh1 expression within DFCs (Fig. 4A). Furthermore, not only protein expression, but also mRNA expression was decreased in *akap12β* morphants (Fig. 4B). These data suggest that the reduced Cdh1 expression within DFCs by *akap12β* downregulation could lead to KV malformation due to DFC fragmentation. Then, we examined how DFC fragmentation affects KV formation in *akap12β* morphants. Interestingly, we identified that the size of KV in DFC *akap12β* morphants was relatively smaller than that of DFC control morphants using differential interference contrast images of living embryos. Consistent with these observations, KV apical lumen area encompassed by Cldn5α was significantly reduced in DFC *akap12β* morphants (0.63-fold vs. DFC control morphants, Fig. 4C, D).

Finally, *akap12β* mRNA was injected with MOs to rescue the phenotypes of *akap12β* morphants. Fragmentation of DFC clusters was restored by exogenous *akap12β*. *Akap12β* mRNA injected *akap12β* morphants showed a higher rate of normally formed single non-fragmented DFC cluster (~76%) than *akap12β* morphants (~57%) (Fig. 4E, F). Consistently, Exogenous *akap12β* mRNA also increased the KV lumen area in *akap12β* morphants (1.75-fold vs. *akap12β* morphants, Fig. 4G, H). Taken together, these data suggest that the loss of cell collectivity within DFCs reduces KV size and this reduction finally results in heart laterality defects in *akap12β* morphants.

DISCUSSION

The current study investigated the role of *akap12β* and *akap12α* in heart laterality establishment, providing the first experimental evidence that *akap12β*, not *akap12α*, might play a role in human heart heterotaxy. We showed that *akap12β* is the major isoform of *akap12* during embryogenesis and is expressed in DFCs, ascendant cells of KV. Knockdown of *akap12β* led to the reduced *cdh1* expression in DFCs which resulted in loss of cell collectivity within DFCs. Finally, fragmented DFC clusters gave rise to smaller KV and malformed KV failed to establish proper heart laterality.

AKAP12 was first identified as an autoantigen in myasthenia gravis, so it was named Gravin (7). In the present study, we investigated the specific role of *akap12β* in heart laterality regulation. In *akap12α* morphants, a single *sox17*:EGFP-positive DFC cluster was preserved and reduction of *cdh1* was not observed during KV development (Supplementary Fig. S2 and S3A, B). In this regard, Gelman *et al*. examined the expression of AKAP12 isoforms in the internal organs including the heart of human and mouse and showed by immunostaining that Akap12 is expressed in the heart during fetal stage (19). Besides, Streb *et al*. reported that *Akap12α* and *Akap12β* are differentially regulated by independent promoters in different tissues and cells (14). In the recent study, two kinds of *de novo* loss of function mutations of AKAP12 within the exon shared by both isoforms were identified as high-risk mutations in CHD patients of left ventricular obstruction and heterotaxy such as dextrocardia, respectively (15). Interestingly, sudden death was observed in 3% to 4% of 4-month-old *Akap12*-null mice which carry the deletion of the common exon of *Akap12* isoforms and cardiomegaly was commonly identified in all those cases by autopsy (20). Accordingly, we hypothesized that *AKAP12α* might control the pure heart development considering it as the major isoform of *AKAP12* in the heart (14) and *AKAP12β* might regulate proper heart positioning depending upon our current investigation, respectively. Further investigation is necessary to define the exact role of *AKAP12* isoforms in heart development.

Our group reported that AKAP12 regulates junctional protein expression such as E-Cadherin, VE-Cadherin, Claudin-1, Occludin, and ZO-1 in diverse systems (8-10, 12). In zebrafish, Cdh1-mediated cell adhesion between adjacent DFCs is essential for their collective migration followed by KV morphogenesis (2, 18). In this regard, we also observed reduction in *cdh1* mRNA and protein expression in *akap12β*-deficient zebrafish. Moreover, exogenous *akap12β* mRNA not only maintained a single non-fragmented DFC cluster and the size of KV but also restored *cdh1* mRNA expression in *akap12β* morphants (Fig. S3C). However, we focused on the role of *akap12β* in the establishment of heart laterality in the current study so further investigations including mechanism(s) of independent expression of *akap12* isoforms and regulation of *cdh1* expression by *akap12β* should be necessary.

Recent studies have revealed that asymmetric distribution of hypoxia contributes to dorsoventral axis establishment during embryogenesis of sea urchin and that retinoic acid (RA) is involved (21-23). Moreover, our group previously reported that partial oxygen pressure regulates AKAP12 expression and that RA induces AKAP12 expression in CNS injury repair (9, 24) and we hypothesized that gradation of such factors could regulate the spatiotemporal expression of *akap12* isoforms. Relating to *cdh1* expression, our group reported that AKAP12 induced by reoxygenation and/or RA suppresses SNAI1, a master transcription factor for epithelial-mesenchymal transition, via the non-Smad pathway during the recovery of CNS injury and that *AKAP12* knockdown increases SNAI1 expression in ARPE-19 epithelial cell line (24). Considering Snai1 as a well-known transcriptional repressor for E-cadherin expression (25) and the possible role(s) of *Snai1* in asymmetric

development (26, 27), we suggest that reduced Cdh1 expression in *akap12β* morphants might be mediated by enhanced Snai1 expression.

In addition to DFC collective migration, DFC numbers and ciliogenesis in KV are crucial for heart laterality (17). Our data indicated that proliferation of DFCs in *akap12β* morphants was comparable with control morphants and the number of cilia in *akap12β* morphants was similar to that in control morphants considering the size of the KV lumen (Supplementary Fig. S4, 5). Malformed KV affected not only heart laterality but also other asymmetric internal organs since we also observed aberrant pancreas positioning in *akap12β* morphants (Supplementary Fig. S6). These data, together with other current data, suggest that loss of function mutation of AKAP12 might be linked to diverse heterotaxy.

Given genetic evidences of *AKAP12* loss of function mutation in certain CHD patients, our data indicating that *akap12β*, not *akap12α*, specifically regulates heart laterality via regulation of *cdh1* expression in DFCs in zebrafish could be extended to the regulation of heart laterality and asymmetric development of internal organs in humans.

MATERIALS AND METHODS

Zebrafish

Tuebingen wild-type zebrafish and transgenic *sox17:egfp*^{S870} zebrafish (Tg(*sox17:egfp*)) were previously described (16). All zebrafish work was carried out in accordance with protocols approved by the Institutional Animal Care and Use Committees of Seoul National University.

Morpholino injection

The protocol of MO injection into zebrafish embryos was previously described (13). Briefly, splice-blocking MOs were injected into the yolk at one-cell stage for whole embryo knockdown or at 128-512-cell stage for DFC-specific knockdown as indicated. Translation-blocking MOs were used to rule out the off-target effects (Supplementary Fig. S7). MOs for *akap12α* and *akap12β* were previously described (13).

In vitro transcription

PCR-amplified *akap12β* was cloned into pCS2+ vector (28). 5′-capped and poly(A)-tailed mRNAs were generated using mMessage mMachine ultra kit (Ambion). 80-120 pg of *akap12β* mRNA was co-injected with *akap12β* MO. Sequences of primers for *akap12β* cloning are summarized in Supplementary Table S1.

RNA isolation and quantitative RT-PCR

The protocols of qRT-PCR and RT-PCR were previously described (29). Total RNA was isolated from zebrafish embryos at indicated stages with TRIzol reagent (Invitrogen) and cDNA was obtained from 2 μg of total RNA using MMLV reverse transcriptase (Promega). qRT-PCR was then performed using StepOnePlus RT-PCR system (Applied Biosystems) with RealHelix qPCR kit (NanoHelix). Relative mRNA expression levels were calculated by the comparative $2^{-\Delta\Delta Ct}$ method. *Actb2* and *eef1a1l1* served as internal controls. Primer sequences for qRT-PCR are summarized in Supplementary Table S1.

Whole-mount ISH and immunostaining

The protocol of ISH was previously described (16). Specific regions of *lefty1* and *foxj1a* were cloned into pGEM T easy vector (Promega). ISH probe vectors for *cmlc1*, *dand5*, *spaw*, and *pan-akap12* were previously described (12, 16) and primer sequences of *lefty1* and *foxj1a* for ISH probe vectors are summarized in Supplementary Table S1. The protocol of whole-mount immunostaining for Tg(*sox17:egfp*) embryos was described previously (16). Mouse anti-Cdh1 (1:200, BD Biosciences) and goat anti-mouse AF546 (1:1000, Invitrogen) were used for immunofluorescence. Stained embryos were mounted in glycerol and images were obtained by an AxioCam ICC-1 camera (Zeiss) on a Stemi 2000C (Zeiss) for immunohistochemistry and an LSM700 confocal microscope (Zeiss) for immunofluorescence, respectively, and processed using ZEN 2012 software (Zeiss).

Statistical analysis

Measurement of KV lumen area was described previously (16). The data are presented as means ± SD and analyzed with Prism 5 (GraphPad Software, Inc.). The data in Fig. 4B and 4D were analyzed by two-tailed Student's *t*-test and the data in Fig. 4H were analyzed by one-way ANOVA test.

ACKNOWLEDGEMENTS

The authors appreciated Emeritus Prof. Kyu-Won Kim (Seoul National University, Seoul, Korea) for mentoring and providing expertise on this study. J.-g.K. designed the research, performed experiments and cared for zebrafish; H.-H.K. analyzed data and helped write the manuscript; S.-J.B. wrote the manuscript and supervised the research. This work was supported by Basic Science Research Program (NRF-2017R1A6A3A11032239) through the NRF funded by the Korean Ministry of Education and the Medical Research Center Program (2014R1A5A20 009936) through the NRF funded by the Korean Ministry of Science, ICT and Future Planning (MSIP).

CONFLICTS OF INTEREST

The authors have no conflicting interests.

REFERENCES

1. Essner JJ, Amack JD, Nyholm MK, Harris EB and Yost HJ (2005) Kupffer's vesicle is a ciliated organ of asymmetry in the zebrafish embryo that initiates left-right development

of the brain, heart and gut. Development 132, 1247-1260
2. Matsui T, Thitamadee S, Murata T et al (2011) Canopy1, a positive feedback regulator of FGF signaling, controls progenitor cell clustering during Kupffer's vesicle organogenesis. Proc Natl Acad Sci U S A 108, 9881-9886
3. Oteiza P, Koppen M, Concha ML and Heisenberg CP (2008) Origin and shaping of the laterality organ in zebrafish. Development 135, 2807-2813
4. Desgrange A, Le Garrec JF and Meilhac SM (2018) Left-right asymmetry in heart development and disease: forming the right loop. Development 145, dev162776
5. van der Linde D, Konings EE, Slager MA et al (2011) Birth prevalence of congenital heart disease worldwide: a systematic review and meta-analysis. J Am Coll Cardiol 58, 2241-2247
6. Hartill VL, van de Hoek G, Patel MP et al (2018) DNAAF1 links heart laterality with the AAA+ ATPase RUVBL1 and ciliary intraflagellar transport. Hum Mol Genet 27, 529-545
7. Gelman IH (2012) Suppression of tumor and metastasis progression through the scaffolding functions of SSeCKS/Gravin/AKAP12. Cancer Metastasis Rev 31, 493-500
8. Choi YK, Kim JH, Kim WJ et al (2007) AKAP12 regulates human blood-retinal barrier formation by downregulation of hypoxia-inducible factor-1alpha. J Neurosci 27, 4472-4481
9. Lee S-W, Kim WJ, Choi YK et al (2003) SSeCKS regulates angiogenesis and tight junction formation in blood-brain barrier. Nat Med 9, 900
10. Cha JH, Wee HJ, Seo JH et al (2014) AKAP12 mediates barrier functions of fibrotic scars during CNS repair. PLoS One 9, e94695
11. Weiser DC, Pyati UJ and Kimelman D (2007) Gravin regulates mesodermal cell behavior changes required for axis elongation during zebrafish gastrulation. Genes Dev 21, 1559-1571
12. Kwon HB, Choi YK, Lim JJ et al (2012) AKAP12 regulates vascular integrity in zebrafish. Exp Mol Med 44, 225-235
13. Kim HH, Kim JG, Jeong J, Han SY and Kim KW (2014) Akap12 is essential for the morphogenesis of muscles involved in zebrafish locomotion. Differentiation 88, 106-116
14. Streb JW, Kitchen CM, Gelman IH and Miano JM (2004) Multiple promoters direct expression of three AKAP12 isoforms with distinct subcellular and tissue distribution profiles. J Biol Chem 279, 56014-56023
15. Jin SC, Homsy J, Zaidi S et al (2017) Contribution of rare inherited and de novo variants in 2,871 congenital heart disease probands. Nat Genet 49, 1593-1601
16. Kim JG, Bae SJ, Lee HS, Park JH and Kim KW (2017) Claudin5a is required for proper inflation of Kupffer's vesicle lumen and organ laterality. PLoS One 12, e0182047
17. Joseph Yost H (1999) Diverse initiation in a conserved left-right pathway? Curr Opin Genet Dev 9, 422-426
18. Tay HG, Schulze SK, Compagnon J et al (2013) Lethal giant larvae 2 regulates development of the ciliated organ Kupffer's vesicle. Development 140, 1550-1559
19. Gelman IH, Tombler E and Vargas J (2000) A Role for SSeCKS, a major protein kinase C substrate with tumour suppressor activity, in cytoskeletal architecture, formation of migratory processes, and cell migration during embryogenesis. Histochem J 32, 13-26
20. Akakura S, Huang C, Nelson PJ, Foster B and Gelman IH (2008) Loss of the SSeCKS/Gravin/AKAP12 gene results in prostatic hyperplasia. Cancer Res 68, 5096-5103
21. Sugrue KF, Sarkar AA, Leatherbury L and Zohn IE (2019) The ubiquitin ligase HECTD1 promotes retinoic acid signaling required for development of the aortic arch. Dis Model Mech 12, dmm036491
22. Vroomans RMA and Ten Tusscher K (2017) Modelling asymmetric somitogenesis: Deciphering the mechanisms behind species differences. Dev Biol 427, 21-34
23. Robichaux JP, Fuseler JW, Patel SS, Kubalak SW, Hartstone-Rose A and Ramsdell AF (2016) Left-right analysis of mammary gland development in retinoid X receptor-alpha+/- mice. Philos Trans R Soc Lond B Biol Sci 371, 20150416
24. Cha JH, Wee HJ, Seo JH et al (2014) Prompt meningeal reconstruction mediated by oxygen-sensitive AKAP12 scaffolding protein after central nervous system injury. Nat Commun 5, 4952
25. Cano A, Pérez-Moreno MA, Rodrigo I et al (2000) The transcription factor snail controls epithelial–mesenchymal transitions by repressing E-cadherin expression. Nat Cell Biol 2, 76-83
26. Gupta K, Pilli VS and Aradhyam GK (2016) Left-right axis asymmetry determining human cryptic gene is transcriptionally repressed by snail. BMC Dev Biol 16, 39
27. Collins MM, Baumholtz AI, Simard A, Gregory M, Cyr DG and Ryan AK (2015) Claudin-10 is required for relay of left-right patterning cues from Hensen's node to the lateral plate mesoderm. Dev Biol 401, 236-248
28. Bae SJ, Shin MW, Kim RH et al (2017) Ninjurin1 assembles into a homomeric protein complex maintained by N-linked glycosylation. J Cell Biochem 118, 2219-2230
29. Bae SJ, Shin MW, Son T et al (2019) Ninjurin1 positively regulates osteoclast development by enhancing the survival of prefusion osteoclasts. Exp Mol Med 51, 7